RSC Advances

PAPER

Cite this: *RSC Adv.*, 2016, **6**, 101578

DBU-catalyzed biobased poly(ethylene 2,5-furandicarboxylate) polyester with rapid melt crystallization: synthesis, crystallization kinetics and melting behavior†

Jiaping Wu,[a] Hongzhou Xie,[a] Linbo Wu,*[a] Bo-Geng Li[a] and Philippe Dubois*[bc]

Received 23rd August 2016
Accepted 19th October 2016

DOI: 10.1039/c6ra21135f

www.rsc.org/advances

Poly(ethylene 2,5-furandicarboxylate) (PEF) is in the spotlight as a new emerging biobased polyester. Usually, PEF exhibits very slow and weak melt crystallization behavior. In this study, PEF synthesis *via* a transesterification polycondensation method catalyzed by 1,8-diazabicyclo[5.4.0]undec-7-ene (DBU) as an organic nonmetallic catalyst was attempted. PEF with a moderate molecular weight (intrinsic viscosity 0.54 dL g^{-1}) and low diethylene glycol furandicarboxylate unit content (DEGF 1.7%) was successfully synthesized and the melt crystallization kinetics and melting behavior were investigated. The DBU-catalyzed PEF exhibited rapid melt crystallization in both nonisothermal and isothermal manners. At cooling rate of 10 °C min^{-1}, a melt crystallization peak appeared around 158 °C with a crystallization enthalpy of 29 J g^{-1}. DSC and WAXD results indicated a crystallinity of 27–34% after sufficient isothermal melt crystallization at 160–210 °C. A minimum of melt crystallization half time, 1.6 min, appeared at 160 °C. The equilibrium melting point of PEF was estimated to be 243 °C.

Introduction

Developing new biobased monomers and polymers from natural renewable biomass resources has drawn great attention from scientists, engineers and government agencies aiming at reducing both fossil fuel consumption and environment pollution.[1–4] 2,5-Furandicarboxylic acid (FDCA) has been proposed as one of the most important building blocks from biomass by the U.S. Department of Energy.[5] Because its properties are comparable to those of petroleum-based terephthalic acid (TPA), it is promising to develop poly(ethylene 2,5-furandicarboxylate) (PEF) and related derivatives as potential substitutes for poly(ethylene terephthalate) (PET). With respect to PET, PEF displays some remarkable performance particularly for packaging applications due to its comparable or even better thermo-mechanical and much better gas barrier properties.[6–8] Moreover, PEF production could reduce non-renewable energy use and the greenhouse gas emission by 40–50% and 45–55%, respectively.[6] Pilot scale manufacture of PEF has been built by Avantium Company (Netherlands) since 2010 and products have been developed for fiber and packaging uses.[6] At labscale level, the synthesis of PEFs *via* different routes and their structure–property relationships have been frequently reported so far.[6,7,9–21] Very recently, Papageorgiou *et al.* reviewed all the research efforts of furanoate polyesters including PEF, from synthesis to thermal and barrier properties.[22]

As a semi-crystalline polymer, the crystallization of PEF has a great effect on its thermo-mechanical properties and further determines its end-use applications. Crystallization and melting behaviors of PEF have been reported by many researchers.[7,8,14–19,21,23] In general, PEF crystallizes even more slowly than PET[18] which was well known for its relatively slow crystallization. Furthermore and similar to PET, PEF crystallized more slowly from the melt than from the glassy state[16] though it was reported that crystal nucleus could be generated from PEF melt even at very small supercooling.[18] van Berkel *et al.*,[20] Stoclet G. *et al.*[23] and Tsanaktsis V. *et al.*[24] reported the isothermal melt crystallization kinetics of PEF. It was found that the crystallization rate of PEF strongly depended on the catalyst used for PEF synthesis and increased with decreasing its molecular weight (M_n 12 000–28 000 Da).[20] PEF with M_n of 5000 Da (used as prepolymer for solid state polycondensation) exhibited rapid isothermal melt crystallization rate, but the crystallization rate of PEF with M_n higher than 10 000 Da proved very slow.[7] The half crystallization time ($t_{1/2}$) at the temperature of maximum crystallization rate (160–170 °C) was reported to be

[a]*State Key Laboratory of Chemical Engineering at ZJU, College of Chemical and Biological Engineering, Zhejiang University, Hangzhou 310027, China. E-mail: wulinbo@zju.edu.cn; Fax: +86-571-87952631; Tel: +86-571-87952631*

[b]*Laboratory of Polymeric and Composite Materials (LPCM), Center of Innovation and Research in Materials and Polymers (CIRMAP), University of Mons, Mons 7000, Belgium. E-mail: philippe.dubois@umons.ac.be*

[c]*Materials Research and Technology Department (MRT), Luxembourg Institute of Science and Technology (LIST), 41 rue du Brill, L-4422 Belvaux, Luxembourg*

† Electronic supplementary information (ESI) available. See DOI: 10.1039/c6ra21135f

16.6–39.1 min,[20] 15 min (ref. 23) and ~8 min (ref. 24) for PEF with M_n of 16 000 Da,[20] 15 000 Da (ref. 23) and 11 200 Da,[24] respectively.

Because of the slow melt crystallization rate, non-isothermal melt crystallization researches of PEF were usually conducted at very slow cooling rate or after self-nucleation. Jiang M. *et al.* reported a weak non-isothermal melt crystallization peak without specific enthalpy around 145 °C when cooled at 5 °C min^{-1}.[15] Codou *et al.* reported non-isothermal melt crystallization kinetics of PEF at cooling rate ranging from 0.5 to 1.5 °C min^{-1}. At such low cooling rates, PEF exhibited apparent melt crystallization peaks at 175–163 °C with high crystallization enthalpy of 45–43 J g^{-1}.[16] Papageorgiou *et al.* reported rapid non-isothermal melt crystallization after self-nucleation.[18] Self-nucleation also resulted in faster isothermal melt crystallization of PEF.[24] Thiyagarajan *et al.* reported rapid non-isothermal melt crystallization of PEF at conventional cooling rate without self-nucleation. Cooling at 10 °C min^{-1}, a melt crystallization peak with a high enthalpy ΔH_c of 43 J g^{-1} was observed around 158 °C.[19] The rapid crystallization might be ascribed to its low diethylene glycol furandicarboxylate (DEGF) unit content (*ca.* 2%). Usually, DEG dicarboxylate unit is easily formed *via* etherification side reaction and its presence is known to affect significantly the so-produced polyester crystallization.[25–29] As such PEFs display poorer crystallizability than PET,[18] synthesis of PEF with low DEGF content is very desirable but it is still a challenge to date. Study of the crystallization kinetics and melting behavior of PEF with high crystallizability is also lacking in literature and needs to be further studied.

On the other hand, metallic catalysts, especially Sb-, Ti- and Sn-based ones are commonly used in polyester synthesis. However, residual metallic catalyst may result in adverse impact on polyester properties like coloration, thermal instability and electrical performance or lead to potential environmental and healthy problems in end-uses. Some of the previous researches showed that the attempt to synthesize PEF by melt polymerization with metallic catalysts resulted in strongly colored polymers with intrinsic viscosities not higher than 0.4–0.5 dL g^{-1}.[22] So it is very desirable to find more ecofriendly catalysts. Researches in the last two decades have indicated that organic non-metallic catalysts can represent efficient candidates for replacing metallic ones in polyester synthesis.[30–35] For examples, creatinine[36,37] and organic sulfonic acids[38] were used as catalysts for polycondensation of lactic acid, and 1,8-diazabicyclo[5.4.0]undec-7-ene (DBU) was studied as catalyst for polyester synthesis in transesterification[39] or solution polymerization.[40] In a recent report, a non-metallic catalyst, 1,4-diazabicyclo[2.2.2]octane (DABCO) was used in ring-opening polymerization of the corresponding cyclic oligomers, oligo(alkylene furandicarboxylate)s, to synthesize PEF and poly(butylene furandicarboxylate) (PBF).[21] But so far there is no report available on PEF synthesis *via* polycondensation as promoted by non-metallic catalyst.

In this study, the DBU-catalyzed PEF synthesis, and the crystallization kinetics and melting behavior of the resulting PEF are reported. PEF was synthesized through melt polycondensation of dimethyl 2,5-furandicarboxylate (DMF) and ethylene glycol (EG) using DBU as a non-metallic catalyst. The chain structure was characterized in details and the non-isothermal and isothermal melt crystallization kinetics and melting behavior of PEF were investigated. Interestingly, using DBU catalyst, PEF with low DEGF content and moderate chain length was successfully synthesized and exhibited reasonably high non-isothermal and isothermal melt crystallization rates. To the best of our knowledge, this is the first report on rapid melt crystallization of PEF synthesized by nonmetallic catalyzed polycondensation.

Results and discussion

Synthesis and characterization

In most reports, PEF was synthesized with metallic catalysts such as Ti-,[7,14,18,19] Sn-[21] and Sb-based[16,17,23] ones and exhibited slow melt crystallization. To avoid potential disadvantageous effect of residual metallic catalysts and to synthesize PEF with good crystallizability, two organic catalysts, namely, 1,8-diazabicyclo[5.4.0]undec-7-ene (DBU) and 1,5,7-triazabicyclo[4.4.0]dec-5-ene (TBD), were tried for PEF synthesis from EG and DMF *via* a two-stage polycondensation process, namely, transesterification followed by melt polycondensation. Some selected metallic catalysts were also used for sake of comparison.

The synthesis conditions and structural molecular characteristics of the synthesized PEFs are listed in Table 1. The DEGF content was determined by ^{1}H NMR spectroscopy. A typical ^{1}H NMR spectrum of a representative PEF synthesized by DBU catalyst is shown in Fig. 1. In addition to the chemical shift of the vinyl protons in the furan ring at 7.46 ppm (a) and the methylene protons in EG structure unit at 4.88 ppm (b), extra chemical shifts were also observed at 4.76 ppm (c) and 4.25 ppm (d). These chemical shifts are attributed to methylene protons in diethylene glycol furandicarboxylate (DEGF) unit, which is formed as by-product from etherification side reaction of EG or hydroxyethyl ester end-groups. Etherification is often catalyzed by acidic substances such diacid monomer and/or catalyst and inevitable in EG-involved polycondensation. It is common in PET synthesis[26–29] and also had been reported in synthesis of PEF[19] and some related copolyesters.[29] From the ^{1}H NMR spectrum, the molar fraction of DEGF unit in PEF (ϕ_{DEGF}) was calculated *via* eqn (1) and the results are listed Table 1. Tetrabutyl titanate (TBT) and stannous oxalate (SnOxa) exhibited high catalytic reactivity but low selectivity (high relative content in DEGF), so PEFs with high intrinsic viscosity ([η] 0.99 and 0.65 dL g^{-1}, respectively) but also high ϕ_{DEGF} (2.99 and 2.47%) were produced. The two Sb-based catalysts, namely, antimony(III) oxide (Sb_2O_3) and ethylene glycol antimony ($Sb_2(EG)_3$), had much better selectivity (ϕ_{DEGF} as low as 0.94 and 1.51%, respectively) but also much poorer catalytic reactivity ([η] 0.46 and 0.40 dL g^{-1}). In comparison with TBT and SnOxa, DBU and TBD led to lower DEGF content (0.50–1.72% *vs.* 2.47–2.99%). Such a good selectivity might be related to the alkalinity of these two amine-based organo-catalysts (pK_a 12, 13.7 for DBU and TBD, respectively[41,42]) as the etherification reaction is known to be promoted by acid-catalysis. Among the two studied organo-

Table 1 PEF synthesis conditions[a], structural molecular characteristics and thermal transition properties of PEFs

Run	EG/DMF	Cat.[b] (%)	$[\eta]^d$ (dL g^{-1})	ϕ_{DEGF}[c] (%)	T_c (°C)	ΔH_c (J g^{-1})	T_g (°C)	T_{cc} (°C)	ΔH_{cc} (J g^{-1})	T_m (°C)	ΔH_m (J g^{-1})
PEF1	2.5	TBT, 0.2	0.99	2.99	ND	ND	91.3	ND	ND	ND	ND
PEF2	2.5	SnOxa, 0.2	0.65	2.47	ND	ND	89.2	ND	ND	ND	ND
PEF3	2.5	Sb_2O_3, 0.1	0.46	0.94	163	36.4	89.8	ND	ND	214	39.7
PEF4	2.5	$Sb_2(EG)_3$, 0.1	0.40	1.51	149	14.1	89.4	161	21.7	216	40.3
PEF5	3.0	DBU, 0.1	0.54	1.71	158	29.3	88.9	ND	ND	212	34.8
PEF6	2.0	TBD, 0.1	0.13	1.72	148	3.2	86.7	174	31.1	216	40.8
PEF7	2.5	TBD, 0.2	0.23	0.50	—	—	—	—	—	—	—

[a] Transesterification at 170–200 °C and then melt polycondensation at 230–240 °C. [b] Cat./DMF molar percentage. [c] Diethylene glycol furandicarboxylate (DEGF) unit content in PEF determined by ^{1}H NMR. [d] Intrinsic viscosity of PEF.

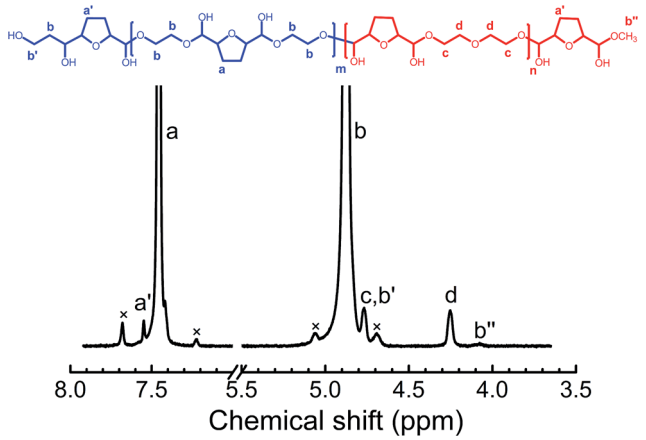

Fig. 1 ^{1}H NMR spectrum (400 MHz, d_1-TFA, 25 °C) of PEF (sample no. 5 in Table 1). The spin side bands are marked as "×".[43]

catalysts, TBD proved to display a rather low catalytic reactivity and therefore only low molecular weight PEFs ([η] 0.13–0.23 dL g^{-1}) were obtained, even at higher TBD loading (0.2 mol%). In comparison, DBU had reasonably good catalytic reactivity and moderate molecular weight PEF ([η] 0.54 dL g^{-1}) was produced at 0.1% loading. In comparison with Sb_2O_3, DBU exhibited slightly lower selectivity (ϕ_{DEGF} 1.71% *vs.* 1.54%) but also slightly higher catalytic reactivity ([η] 0.54 dL g^{-1} *vs.* 0.46 dL g^{-1}).

$$\text{DEGF\%} = A_d/(A_d + A_b) \times 100\% \quad (1)$$

Non-isothermal melt crystallization kinetics and melting behavior

It is noteworthy that the presence of diethylene glycol terephthalate (DEGT) unit in PET results in a significant decrease of crystallizability and melting temperature but also affects the mechanical properties and thermal and hydrolytic stability.[25] As non-isothermal melt crystallization always takes place during industrial melt processes such as extrusion, injection, mold pressing and melt spinning process, it is highly desirable to understand the melt crystallization behavior of PEF, particularly with low DEGF content, so as to improve processability and enhance the thermo-mechanical performance of the related materials.

Non-isothermal melt crystallization and subsequent melting behavior of PEF samples synthesized with different catalysts were compared under standard heating–cooling–heating cycle at heating/cooling rate of 10 °C min^{-1}. The DSC curves are shown in Fig. 2 and the transition properties are summarized in Table 1. All the samples showed glass transition temperature (T_g, 86.7–91.3 °C) higher than PET (76 °C (ref. 8)), especially for the high IV sample catalyzed by TBT (91.3 °C) as the T_g showed an increasing tendency with intrinsic viscosity increasing. The Sb_2O_3-catalyzed PEF showed an intensive crystallization peak

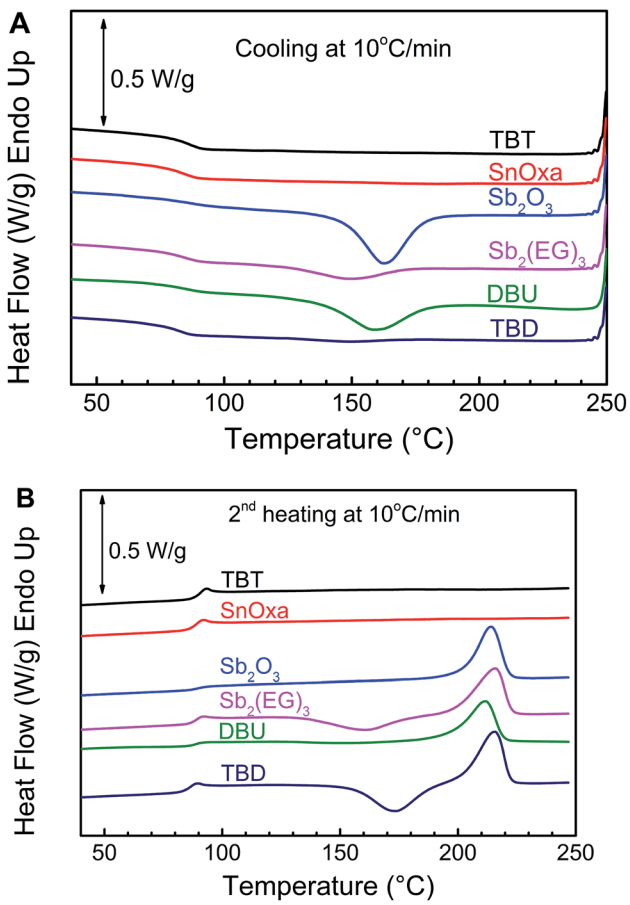

Fig. 2 (A) Cooling and (B) 2nd heating DSC curves of PEF samples synthesized with different catalysts (heating and cooling rate: 10 °C min^{-1}).

with a crystallization enthalpy (ΔH_c) of 36.4 J g^{-1} at 163 °C upon cooling, no cold crystallization and an important melting peak with a melting enthalpy (ΔH_m) of 39.7 J g^{-1} at 214 °C upon second heating, indicating reasonably good crystallizability. When $Sb_2(EG)_3$ was used as catalyst instead, the resultant PEF exhibited clearly weaker melt crystallizability: smaller ΔH_c (14.1 J g^{-1}), lower T_c (149 °C) and cold crystallization peak upon second heating. The TBT- and SnOxa-catalyzed PEFs showed neither melt crystallization peak upon cooling nor cold crystallization and melting peaks at first and second heating, suggesting that they crystallized very slowly or were nearly amorphous. The DBU-catalyzed PEF crystallized at 158 °C from melt with a ΔH_c of 29.3 J g^{-1}, and melt at 212 °C with a ΔH_m of 34.8 J g^{-1}, without cold crystallization upon second heating. The values of ΔH_c, ΔH_m and T_c were slightly lower than those of the Sb_2O_3-catalyzed PEF, possibly due to higher DEGF content and molecular weight. The crystallinity estimated from the ΔH_c against the fusion heat of the completely crystallized PEF (140J g^{-1})[18] is 21% *vs.* 26% for the DBU- and Sb_2O_3-catalyzed PEF, respectively. From these results, it can be concluded that the DBU-catalyzed PEF has reasonably good melt crystallizability close to Sb_2O_3-catalyzed PEF at cooling rate of 10 °C min^{-1}. However, the TBD-catalyzed PEF (PEF7) only exhibited a weak melt crystallization peak with a ΔH_c of 3.2 J g^{-1} at 148 °C though it has lower DEGF content (0.5%) and molecular weight (0.23 dL g^{-1}). This suggests that residual catalyst might be a third factor besides ϕ_{DEGF} and molecular weight to affect PEF crystallization. Further studies on what factors influence PEF crystallization are still under way and will be reported later on.

Above results indicated that DBU-catalyzed PEF melt crystallized more quickly than other PEFs except the Sb_2O_3-catalyzed one at routine cooling rate of 10 °C min^{-1}. To better understand its melt crystallization behavior, non-isothermal melt crystallization at various cooling rates was further studied. DSC curves of PEF at cooling rates ranging from 5 to 25 °C min^{-1} and second heating rate of 10 °C min^{-1} are shown in Fig. 3. The thermal transition properties are summarized in Table 2. As expected, the melt crystallization peak of PEF shifted to lower temperature (from 171 to 148 °C) and the ΔH_c decreased from 41.2 J g^{-1} to 3.7 J g^{-1} with increasing cooling rate. At cooling rate of 5–10 °C min^{-1}, the PEF sample exhibited melt crystallization peaks around 171–158 °C with ΔH_c of 41–29 J g^{-1} (or crystallinity 30–21%). In the second heating, PEF did not cold-crystallize and melt at 212–213 °C with ΔH_m of 41.7–34.8 J g^{-1}. At higher cooling rate (15–25 °C min^{-1}), PEF exhibited clearly lower T_c (151–148 °C) and ΔH_c (15.3–3.7 J g^{-1}) values. In the second heating, cold crystallization peaks appeared around 154–159 °C with crystallization enthalpy of 13–23 J g^{-1}, and PEF melted around 211 °C with ΔH_m of 34–31 J g^{-1}. These results indicated that the DBU-catalyzed PEF possesses rapid and complete melt crystallization at cooling rate lower than or equal to 10 °C min^{-1}, while retained some crystallizability up to certain extent at higher cooling rate.

Avrami equation is widely used in isothermal crystallization kinetics of polymers.[44,45] It expresses the time-evolution of relative crystallinity as shown in eqn (2), where X_t, k and n are the relative crystallinity degree, crystallization rate constant and

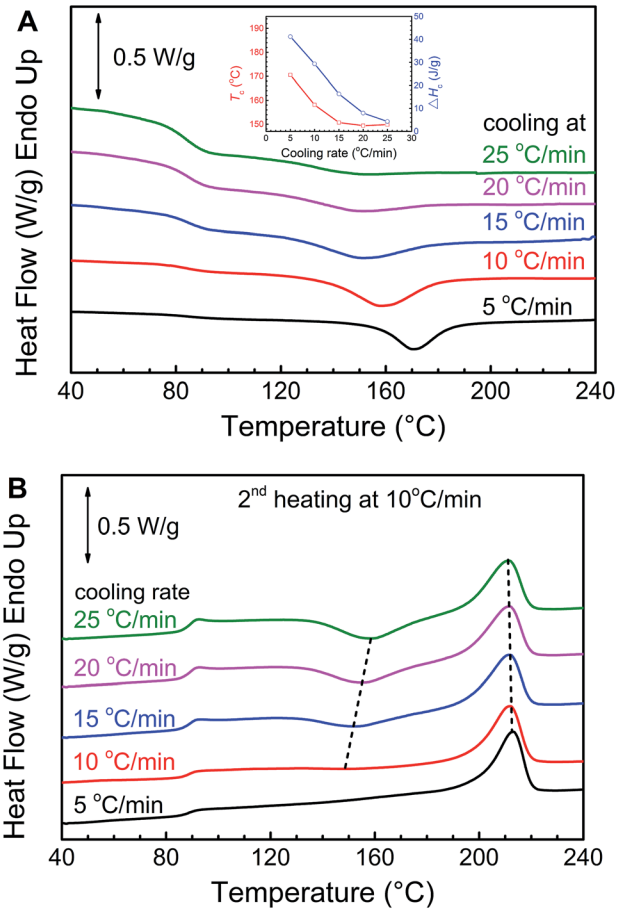

Fig. 3 (A) Cooling scan DSC curves of the DBU-catalyzed PEF at various cooling rates and (B) the consequent second heating scan curves at 10 °C min^{-1}.

Avrami exponent, respectively. Jeziorny *et al.* used it (eqn (3)) to analyze non-isothermal crystallization kinetics through a temperature–time conversion by the eqn (4) in which T_0, T and C were the onset crystallization temperature, the crystallization temperature at time t and the cooling rate, respectively.[44] Some of the analyzed results are illustrated in Fig. S1 and S2.† The obtained crystallization rate constant k was modified by cooling rate to get a corrected crystallization rate constant (k') and half crystallization time ($t'_{1/2}$), see eqn (5) and (6). In this study, the non-isothermal melt crystallization kinetics of PEF was analyzed with Jeziorny's method. The fitted curves are shown in Fig. 4, and the related equations and the parameters obtained from these fittings are summarized in Table 3.

$$\log[-\ln(1 - X_t)] = \log k + n \log t \quad (2)$$

$$\log[-\ln(1 - X_t)] = \log k + n' \log t \quad (3)$$

$$t = (T_0 - T)/C \quad (4)$$

$$\log k' = \log k/C \quad (5)$$

$$t_{1/2} = (\ln 2/k')^{1/2} \quad (6)$$

Table 2 Thermal transition data of non-isothermal melt crystallization at different cooling rates and second heating at 10 °C min^{-1} of the DBU-catalyzed PEF

Cooling rate (°C min^{-1})	Cooling scan			2nd heating scan at 10 °C min^{-1}				
	T_c (°C)	ΔH_c (J g^{-1})	X_c[a] (%)	T_g (°C)	T_{cc} (°C)	ΔH_{cc} (J g^{-1})	T_m (°C)	ΔH_m (J g^{-1})
5.0	170.5	41.2	30.1	88.6	ND	ND	213	41.7
10.0	158.1	29.3	21.4	88.6	ND	ND	212	34.8
15.0	150.7	15.3	11.2	89.7	153.5	12.5	211	33.8
20.0	149.4	8.0	5.8	89.5	156.1	20.7	211	32.0
25.0	147.6	3.7	2.7	89.6	159.1	22.8	211	31.3

[a] Estimated from the ratios of the measured crystallization enthalpy ΔH_c and the melting enthalpy ΔH_m (140 J g^{-1}) of the completely crystallized PEF.[23]

Table 3 Fitting results of non-isothermal melt crystallization of the DBU-catalyzed PEF at various cooling rates with Jeziorny method

Parameters	Cooling rate (°C min^{-1})				
	5	10	15	20	25
n'	2.5	2.4	2.3	2.2	2.1
k' (min$^{-n'}$)	0.278	0.635	0.810	0.896	0.959
$t_{1/2}$ (min)	1.58	1.04	0.92	0.88	0.85
R^2	0.982	0.993	0.999	0.998	0.999

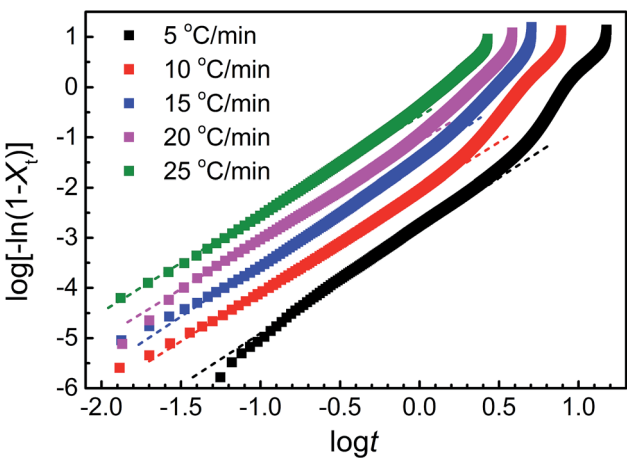

Fig. 4 Kinetic analyses (Jeziorny plots: log[−ln(1 − X_t)] *vs.* log t) of non-isothermal melt crystallization of the DBU-catalyzed PEF at various cooling rates.

The Jeziorny method described the non-isothermal melt crystallization kinetics quite well at the early stage in which the primary crystallization occurred at higher temperature. At the given cooling rates, the log[−ln(1 − X_t)] increase with log t linearly ($R^2 > 0.982$). However, a positive deviation was observed at relatively lower temperature though negative deviation often occurs in crystalline polymers. Such positive deviation may be related to spherulite impingement and secondary crystallization and was also reported in some literatures.[3,46] The Avrami parameter n' lies between 2.1–2.5, suggesting heterogeneous nucleation and two to three dimensional growth of PEF. The corrected crystallization rate constant k' increases and the half crystallization time $t_{1/2}$ decreases with increasing cooling rate. When the cooling rate increased, the crystallization temperature shifted more rapidly to lower temperature, so the supercooling increased and the crystallization rate increased.

Isothermal melt crystallization kinetics and melting behavior

The isothermal crystallization kinetics at crystallization temperature (T_c) ranging from 160 °C to 210 °C was further studied with DSC. The DSC thermograms are shown in Fig. 5A. The exothermic peak of isothermal crystallization broadened, indicating the crystallization rate slowed down with increasing T_c in the experimental range. The crystallization enthalpy ΔH_c reached 40 J g^{-1} after sufficient isothermal crystallization at 160 °C. Comparable values were reported by van Berkel for PEFs synthesized without any catalyst[20] or Stoclet synthesized with Sb_2O_3 catalyst.[23] When a binary catalyst, *i.e.* $Ca(Ac)_2 + Sb_2O_3$, was used, PEF exhibited a higher ΔH_c (50 J g^{-1}), which was ascribed to the nucleation effect of $Ca(Ac)_2$.[20]

The isothermal crystallization kinetics was treated with Avrami equation. The Avrami plots are shown in Fig. S3† and 5B, and the Avrami parameters n and k are summarized in Table 4. It can be seen that Avrami equation fits the isothermal crystallization kinetics quite well in the initial linear part of the curves, which was used for estimating the Avrami parameters. The deviation after the linear part is attributed to secondary crystallization.[47] As an indicator reflecting the nucleation mechanism and crystal growth process of polymers,[48] the Avrami exponent n nearly keeps constant (2.5) and is almost independent of temperature. The n value suggests that PEF might follow either two-dimensional growth with homogeneous nucleation or three-dimensional growth with heterogeneous nucleation.

As expected, the crystallization rate constant decreases and the crystallization half time ($t_{1/2}$) increases exponentially with increasing T_c from 160 °C to 210 °C, see the inserted plots in Fig. 5B. The minimum $t_{1/2}$ value, 1.6 min, appears at 160 °C. It is comparable to the $t_{1/2}$ value (~1.5 min) of PEF (TBT as catalyst, M_n 11 200 g mol^{-1}, [η] 0.45 dL g^{-1}) isothermally melt-crystallized at 160 °C after self-nucleation.[18,24] Clearly, self-nucleation pre-treatment promoted PEF crystallization. Without self-nucleation, the PEF isothermally crystallized from

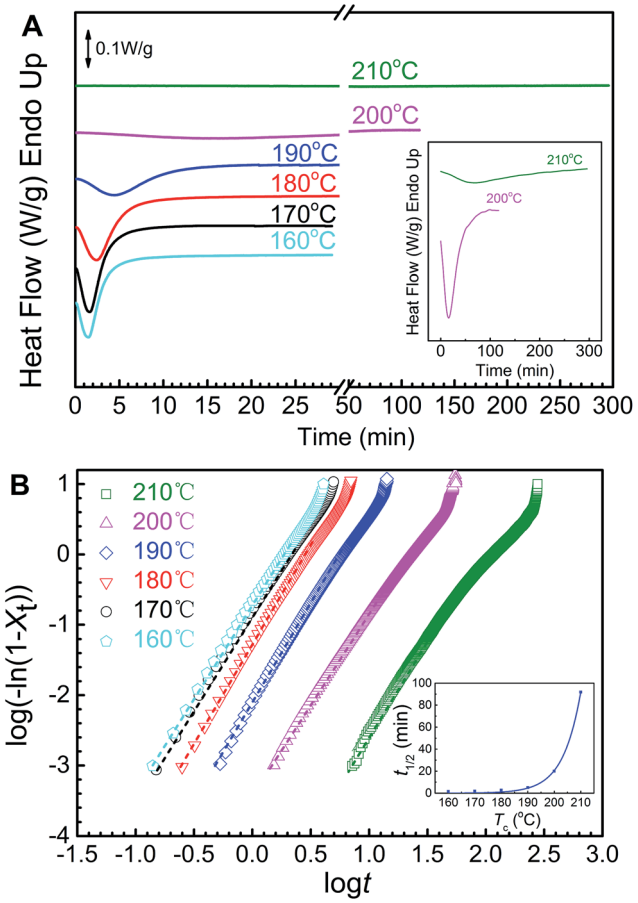

Fig. 5 (A) DSC isothermal melt crystallization curves (the inserted are isothermal crystallization curves at 200 °C and 210 °C) and (B) Avrami plots of isothermal melt crystallization kinetics of the DBU-catalyzed PEF at various crystallization temperatures (dashed lines are fitted curves; the inserted is the half crystallization time *vs.* crystallization temperature plot).

melt much more slowly, with a $t_{1/2}$ value of about 8 min.[24] In comparison, in van Berkel *et al.*'s report,[20] the $t_{1/2}$ value was 18.2 min at 160 °C for PEF (M_n 12 000 g mol^{-1}) synthesized without catalyst; and in Stoclet *et al.*'s report,[23] the minimum $t_{1/2}$ value was about 15 min at 165 °C for a reactor-grade PEF sample (M_n 15 000 g mol^{-1}) synthesized with Sb_2O_3 catalyst. The results indicate that DBU-catalyzed PEF in this study has faster crystallization rate. It has been reported that the crystallization of PEF is influenced by molecular weight: lower molecular weight leads to rapider PEF crystallization.[20] As the intrinsic viscosity of the DBU-catalyzed PEF (0.54 dL g^{-1}) is higher than that of the previously reported one (0.45 dL g^{-1},[18,24] DEGF content data not reported), it can be deduced that the DBU-catalyzed PEF has rapider melt crystallization due to its low DEGF content.

After isothermal melt crystallization, the samples were reheated to 250 °C at 10 °C min^{-1}. In the second heating scan (Fig. 6A), all samples exhibited no cold crystallization peak but two endothermal melting peaks, denoted as peaks I and II. The corresponding melting points and enthalpies are denoted as $T_{m,I}$ and $T_{m,II}$, $\Delta H_{m,I}$ and $\Delta H_{m,II}$, respectively. Similar double melting peaks were also observed by van Berkel *et al.*[20] and Stoclet *et al.*[23] in the same crystallization temperature range. After isothermally crystallization at lower temperature, three melting peaks appeared in the second heating scan.[20] According to Stoclet *et al.*'s report,[23] peak I is ascribed to melting of secondary crystals that consist in small and imperfect crystals, while peak II is attributed to melting of primary crystals formed during the crystallization at T_c. Both peaks shift to higher temperature with T_c. The value of $\Delta H_{m,I}$ keeps unchanged while the value of $\Delta H_{m,II}$ increases slightly with T_c. The sum of $\Delta H_{m,I}$ and $\Delta H_{m,II}$ ranges from 37.3 to 47.9 J g^{-1}, and the crystallinity calculated therefrom ranges from 26.6 to 34.2%.

The plots of the observed melting points, $T_{m,I}$ and $T_{m,II}$ *versus* T_c are shown in Fig. 6B. Both $T_{m,I}$ and $T_{m,II}$ raise linearly with T_c in the experimental range, and $T_{m,I}$ keeps about 10 °C higher than T_c. $T_{m,I}$ shows more pronounced T_c dependence than $T_{m,II}$ does, indicating that peak I relates to the presence of less perfect secondary crystals.[18] According to the well-known Hoffman–Week's equation (eqn (7), in which β is the ratio of the thickness of the final crystallites L_c to that of the preliminary ones L_c^*), the equilibrium melting point (T_m^0) can be obtained as the intercept of the $T_{m,II}$–T_c line with the diagonal line ($T_m = T_c$).

Table 4 Avrami parameters of the DBU-catalyzed PEF isothermally melt crystallized at various crystallization temperatures and the thermal transition properties in subsequent melting at heating rate of 10 °C min^{-1}[a]

	Crystallization temperature, T_c (°C)					
Avrami parameters	160	170	180	190	200	210
n	2.5	2.5	2.5	2.5	2.4	2.4
k (min^{-n} × 10^3)	208	166	57.5	11.0	0.524	0.013
$t_{1/2} = (\ln 2/k)^{1/n}$ (min)	1.6	1.8	2.7	5.1	20.0	5.16
R^2	0.999	0.999	0.999	0.999	0.999	0.996
$T_{m,I}$ (°C)	171.5	179.5	190.6	197.5	214.8	223.8
$T_{m,II}$ (°C)	210.4	211.1	213.9	216.3	221.8	228.3
$\Delta H_{m,total}$ (J g^{-1})	37.3	38.9	42.1	45.6	46.9	47.9
X_c (%)	26.6	27.8	30.1	32.6	33.5	34.2

[a] Estimated from the ratio of the measured melting enthalpy $\Delta H_{m,total}$ ($=\Delta H_{m,I} + \Delta H_{m,II}$) to the fusion heat (140 J g^{-1}) of the completely crystallized PEF.[23]

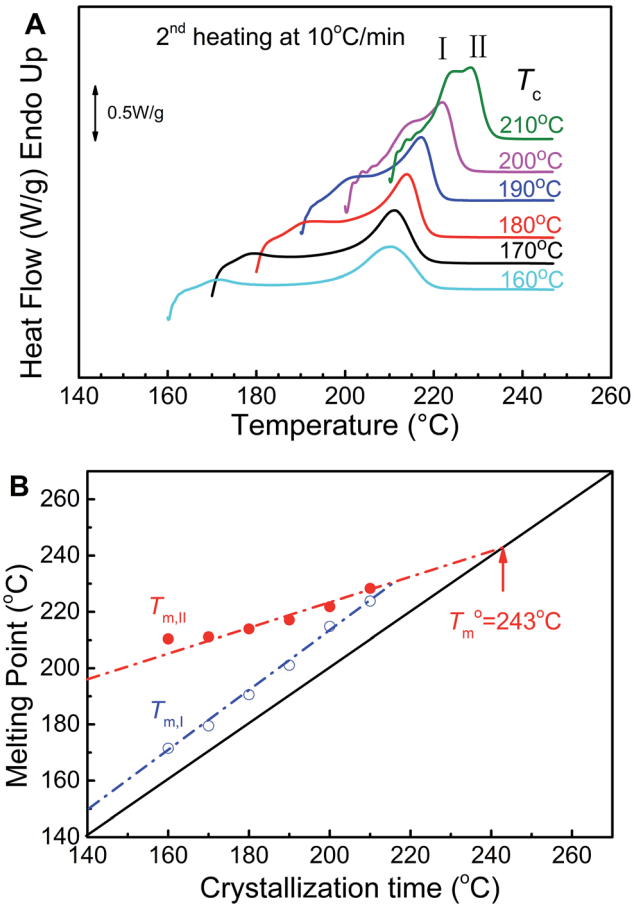

Fig. 6 (A) DSC second heating curves of the DBU-catalyzed PEF at heating rate of 10 °C min^{-1} after isothermal melt crystallization at indicated T_c and (B) Hoffman–Weeks plots to estimate of the equilibrium melting point (T_m^0). Note: the $T_{m,II}$ data at T_c of 160 °C was not used in the linear fitting.

The $T_{m,II}$ data at T_c of 160 °C was not used in the linear fitting as this data is high and not in line with the rest due to crystal reorganization on heating.[23] The T_m^0 of PEF was estimated to be 243 °C. It is close to the results reported by Sbirrazzuoli *et al.*[16] (247 °C) and Knoop *et al.*[7] (240 °C). Higher (265 °C [18]) and lower (226 °C [22]) T_m^0 values were also reported in literatures.

$$T_m = T_m^0(1 - 1/(2\beta)) + T_c/(2\beta) \quad (7)$$

The WAXD pattern of the DBU-catalyzed PEF was recorded after isothermal melt crystallization at 170 °C for 3 h. From the profile shown in Fig. 7, the main sharp peaks appear at 16.4°, 18.1°, 19.6°, 20.8°, 23.7° and 26.9°. The WAXD pattern is similar to those reported previously,[16,20] suggesting that DBU-catalyzed PEF has the same crystalline structure than PEFs synthesized with other catalysts. The pattern was analyzed by peak-fitting in order to obtain the ratio of the total area of all crystalline reflexes to that of all reflexes. The calculated crystallinity is 28.1%, which matches the DSC result (27.8%).

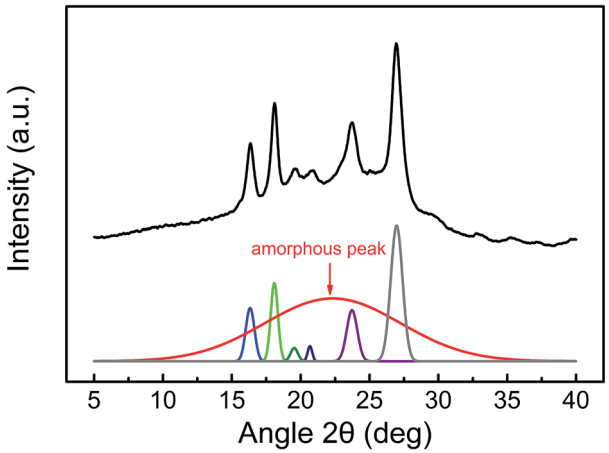

Fig. 7 WAXD diffraction pattern of the DBU-catalyzed PEF melt crystallized at 170 °C for 3 h.

Conclusions

In this study, DBU was tried for the first time as an organic nonmetallic catalyst to synthesize biobased polyester poly(ethylene furandicarboxylate) (PEF) *via* transesterification polycondensation method. PEF with moderate molecular weight (intrinsic viscosity 0.54 dL g^{-1}) and low diethylene glycol furandicarboxylate unit content (DEGF 1.7%) was successfully synthesized and exhibited rapid melt crystallization in both nonisothermal and isothermal manners. At cooling rate of 10 °C min^{-1}, it crystallized directly from melt with a 29 J g^{-1} crystallization peak around 158 °C; in the second heating, there appeared no cold crystallization peak but a 35 J g^{-1} melting peak around 212 °C. After sufficient isothermal melt crystallization at 160–210 °C, the crystallinity reached 27–34%. A minimum of crystallization half time, 1.6 min, appeared at 160 °C. To our best knowledge, this is the shortest melt crystallization half time reported for PEF without self-nucleation. Besides, the equilibrium melting point of PEF was estimated to be 243 °C.

Experimental

Materials

Dimethyl 2,5-furandicarboxylate (DMF, 99.8%, Satar Chem. Co., China), ethylene glycol (EG, 99.0%, Sigma), 1,8-diazabicyclo [5.4.0]undec-7-ene (DBU, 99.0%, Aldrich), 1,5,7-triazabicyclo [4.4.0]dec-5-ene (TBD, 98.0%, J&K Chem. Ltd.), tetrabutyl titanate (TBT, 99.0%, J&K Chemical Ltd.), stannous oxalate (SnOxa, 98.0%, Alfa Aesar), antimony(III) oxide (Sb_2O_3, 99.0%, Sinopec Yizheng Chemical Ltd.) and ethylene glycol antimony ($Sb_2(EG)_3$, self-synthesized) were used without further purification. 1,1,2,2-Tetrachloroethane (TCE), phenol and deuterated trifluoroacetic acid (d_1-TFA) were all purchased from Sinopharm and used as received.

Synthesis of PEF

PEF was synthesized *via* a two-stage transesterification polycondensation method. The monomers DMF and EG (molar

ratio DMF : EG 1 : 2.5–3) and a catalyst (0.1–0.2 mol% of DMF) were charged into a 25 mL flask. After nitrogen purging, the reaction mixture was heated and the transesterification reaction was carried out at 170–200 °C for 6–8 h. When the theoretical amount of the side product, *i.e.*, CH_3OH, was collected, the reaction pressure was reduced to remove the excessive EG. Then, the temperature was raised to 230 °C and the pressure was further reduced to about 100 Pa in about half an hour. The polycondensation reaction was conducted at 230 °C for 3.25 h and then at 240 °C for additional 1.25 h under about 100 Pa. Finally, the obtained PEF polyester was dried in vacuum for characterization.

Characterization

The intrinsic viscosity was measured at 25 °C with an automatic viscosity tester (ZONWON IVS300, China) equipped with a Ubbelohde viscometer, using a mixed phenol/TCE (3/2, w/w) solvent. ^{1}H NMR spectrum was recorded on Bruker AC-80 (400 M). d_1-TFA was used as solvent and tetramethylsilane as internal reference.

Wide angle X-ray diffraction patterns (WAXD) was recorded using a PANalytical X'Pert X-ray diffraction system (PANalytical Company) with CuKα radiation (1.54 Å), working at 40 kV and 40 mA. The sample was scanned from $2\theta = 5°$ to $2\theta = 60°$ with a step size of 0.026° and an acquisition time of 30 s per step.

Crystallization and melting behavior were recorded with differential scanning calorimetry (DSC) on a TA-Q200 thermal analyzer. The calorimetry was calibrated with indium standard. For non-isothermal melt crystallization and melting, a sample of 6–7 mg was heated to 250 °C at a heating rate of 10 °C min^{-1} and kept for 5 min in order to erase its thermal history. The melt was cooled to 30 °C at the rate of 5–25 °C min^{-1} and then kept at this temperature for 3 min. Finally, the sample was heated to 250 °C at 10 °C min^{-1}. For isothermal melt crystallization and melting, a sample was heated to 250 °C and kept for 5 min, then cooled rapidly to the crystallization temperature (160–210 °C) and held at this temperature for enough time (30 min at 160–190 °C, 120 min at 200 °C and 300 min at 210 °C) in order to crystallize completely. At last, it was re-heated to 250 °C at 10 °C min^{-1}.

Acknowledgements

This work was supported by the National Natural Science Foundation of China (51373152), State Key Laboratory of Chemical Engineering (No. SKL-ChE-15D01), the Fundamental Research Funds for the Central Universities (2011FZA4024), the National Key Research and Development Program (2016YFB0302402) and 151 Talents Project of Zhejiang Province.

Notes and references

1 M. Scandola, M. L. Focarete, G. Adamus, W. Sikorska, I. Baranowska, S. Swierczek, M. Gnatowski, M. Kowalczuk and Z. Jedlinski, *Macromolecules*, 1997, **30**, 2568–2574.
2 T. Nie, Y. Zhao, Z. Xie and C. Wu, *Macromolecules*, 2003, **36**, 8825–8829.
3 Z. Su, W. Guo, Y. Liu, Q. Li and C. Wu, *Polym. Bull.*, 2009, **62**, 629–642.
4 S. Inkinen, M. Hakkarainen, A. C. Albertsson and A. Södergård, *Biomacromolecules*, 2011, **12**, 523–532.
5 T. Werpy, G. Petersen, A. Aden, J. Bozell, J. Holladay, J. White, A. Manheim, D. Elliot, L. Lasure and S. Jones, *Top Value Added Chemicals from Biomass Volume I: Results of Screening for Potential Candidates from Sugars and Synthesis Gas*, 2004.
6 E. d. Jong, M. A. Dam, L. Sipos and G. J. M. Gruter, in *Biobased Monomers, Polymers, and Materials*, ed. M. Smith, ACS, Washington DC, 2012, vol. 1105, pp. 1–13.
7 R. J. I. Knoop, W. Vogelzang, J. van Haveren and D. S. van Es, *J. Polym. Sci., Part A: Polym. Chem.*, 2013, **51**, 4191–4199.
8 S. K. Burgess, J. E. Leisen, B. E. Kraftschik, C. R. Mubarak, R. M. Kriegel and W. J. Koros, *Macromolecules*, 2014, **47**, 1383–1391.
9 J. Moore and J. Kelly, *Macromolecules*, 1978, **11**, 568–573.
10 A. Gandini, A. J. D. Silvestre, C. P. Neto, A. F. Sousa and M. Gomes, *J. Polym. Sci., Part A: Polym. Chem.*, 2009, **47**, 295–298.
11 M. G. Gomes, A. Gandini and A. J. D. Silvestre, *J. Polym. Sci., Part A: Polym. Chem.*, 2011, **49**, 3759–3768.
12 D. Lan, H. Yin, W. Dong, M. Chen, T. Li and Z. Ni, *Eng. Plast. Appl.*, 2011, **39**, 17–19.
13 S. S. Baek, M. J. Kim, O. Y. Kim, D. W. Kang, H. J. Kang, K. U. Jeong and S. H. Hwang, *Amer. Chem. Soc.*, 2012, **243**, 379–380.
14 M. Jiang, Q. Liu, Q. Zhang, C. Ye and G. Zhou, *J. Polym. Sci., Part A: Polym. Chem.*, 2012, **50**, 1026–1036.
15 M. Jiang, Q. Liu, Y. Li, Q. Zhang and G. Zhou, *Acta Polym. Sin.*, 2013, **1**, 24–29.
16 A. Codou, N. Guigo, J. van Berkel, E. de Jong and N. Sbirrazzuoli, *Macromol. Chem. Phys.*, 2014, **215**, 2065–2074.
17 P. Gopalakrishnan, S. Narayan-Sarathy, T. Ghosh, K. Mahajan and M. N. Belgacem, *J. Polym. Res.*, 2014, **21**, 1–9.
18 G. Z. Papageorgiou, V. Tsanaktsis and D. N. Bikiaris, *Phys. Chem. Chem. Phys.*, 2014, **16**, 7946–7958.
19 S. Thiyagarajan, W. Vogelzang, R. J. Knoop, A. E. Frissen, J. van Haveren and D. S. van Es, *Green Chem.*, 2014, **16**, 1957–1966.
20 J. G. van Berkel, N. Guigo, J. J. Kolstad, L. Sipos, B. Wang, M. A. Dam and N. Sbirrazzuoli, *Macromol. Mater. Eng.*, 2015, **300**, 466–474.
21 J. Carlos Morales-Huerta, A. Martínez de Ilarduya and S. Muñoz-Guerra, *Polymer*, 2016, **87**, 148–158.
22 G. Z. Papageorgiou, D. G. Papageorgiou, Z. Terzopoulou and D. N. Bikiaris, *Eur. Polym. J.*, 2016, **83**, 202–229.
23 G. Stoclet, G. Gobius du Sart, B. Yeniad, S. de Vos and J. M. Lefebvre, *Polymer*, 2015, **72**, 165–176.
24 V. Tsanaktsis, D. G. Papageorgiou, S. Exarhopoulos, D. N. Bikiaris and G. Z. Papageorgiou, *Cryst. Growth Des.*, 2015, **15**, 5505–5512.

25 J. M. Besnoin and K. Y. Choi, *J. Macromol. Sci., Rev. Macromol. Chem. Phys.*, 1989, **29**, 55–81.
26 L. Finelli, C. Lorenzetti, M. Messori, L. Sisti and M. Vannini, *J. Appl. Polym. Sci.*, 2004, **92**, 1887–1892.
27 H. A. Lecomte and J. J. Liggat, *Polym. Degrad. Stab.*, 2006, **91**, 681–689.
28 W. Romão, M. F. Franco, Y. E. Corilo, M. N. Eberlin, M. A. S. Spinacé and M.-A. De Paoli, *Polym. Degrad. Stab.*, 2009, **94**, 1849–1859.
29 A. F. Sousa, M. Matos, C. S. R. Freire, A. J. D. Silvestre and J. F. J. Coelho, *Polymer*, 2013, **54**, 513–519.
30 R. Nagahata, J. I. Sugiyama, M. Goyal, M. Asai, M. Ueda and K. Takeuchi, *J. Polym. Sci., Part A: Polym. Chem.*, 2000, **38**, 3360–3368.
31 A. F. Sousa, A. Gandini, A. J. Silvestre and C. Pascoal Neto, *ChemSusChem*, 2008, **1**, 1020–1025.
32 M. Sokolsky-Papkov, R. Langer and A. J. Domb, *Polym. Adv. Technol.*, 2011, **22**, 502–511.
33 A. F. Sousa, A. Gandini, A. J. Silvestre, C. P. Neto, J. J. Cruz Pinto, C. Eckerman and B. Holmbom, *J. Polym. Sci., Part A: Polym. Chem.*, 2011, **49**, 2281–2291.
34 A. F. Sousa, A. J. Silvestre, A. Gandini and C. P. Neto, *High Perform. Polym.*, 2012, 1–5.
35 R. Todd, S. Tempelaar, G. Lo Re, S. Spinella, S. A. McCallum, R. A. Gross, J.-M. Raquez and P. Dubois, *ACS Macro Lett.*, 2015, **4**, 408–411.
36 W. Jiang, W. Huang, N. Cheng, Y. Qi, X. Zong, H. Li and Q. Zhang, *Polymer*, 2012, **53**, 5476–5479.
37 W. Huang, N. Cheng, Y. Qi, T. Zhang, W. Jiang, H. Li and Q. Zhang, *Polymer*, 2014, **55**, 1491–1496.
38 B. Peng, Y. Xu, J. Hu, Z. Bu, L. Wu and B. G. Li, *Polym. Degrad. Stab.*, 2013, **98**, 1784–1789.
39 P. A. Fokou and M. A. Meier, *Macromol. Rapid Commun.*, 2008, **29**, 1620–1625.
40 T. Nishikubo and K. Ozaki, *Polym. J.*, 1990, **22**, 1043–1050.
41 D. Granitza, M. Beyermann, H. Wenschuh, H. Haber, L. A. Carpino, G. A. Truran and M. Bienert, *J. Chem. Soc., Chem. Commun.*, 1995, 2223–2224.
42 V. Verdolino, R. Cammi, B. H. Munk and H. B. Schlegel, *J. Phys. Chem. B*, 2008, **112**, 16860–16873.
43 J. Ma, X. Yu, J. Xu and Y. Pang, *Polymer*, 2012, **53**, 4145–4151.
44 A. Jeziorny, *Polymer*, 1978, **19**, 1142–1144.
45 N. Bosq, N. Guigo, E. Zhuravlev and N. Sbirrazzuoli, *J. Phys. Chem. B*, 2013, **117**, 3407–3415.
46 W. Limwanich, S. Phetsuk, P. Meepowpan, N. Kungwan and W. Punyodom, *Chiang Mai Journal of Science*, 2016, **43**, 329–338.
47 S. W. Lee, M. Ree, C. E. Park, Y. K. Jung, C. S. Park, Y. S. Jin and D. C. Bae, *Polymer*, 1999, **40**, 7137–7146.
48 M. Avrami, *J. Chem. Phys.*, 1939, **7**, 1103–1112.